Efficient Numerical Shadowing Global Error Estimation for High Dimensional Systems

by
Jon Collis

ProQuest LLC.
789 East Eisenhower Parkway
P.O. Box 1346
Ann Arbor, MI 48106 – 1346

A thesis submitted to the Faculty and the Board of Trustees of the Colorado School of Mines in partial fulfillment of the requirements for the degree of Master of Science (Mathematical and Computer Sciences).

Golden, Colorado
Date 19 June, 2003

Signed: _____
Jon Collis

Approved: _____
Dr. Erik Van Vleck
Mathematical and Computer Sciences
Thesis Advisor

Approved: _____
Dr. Paul Martin
Mathematical and Computer Sciences
Thesis Co-Advisor

Golden, Colorado
Date 19 June 2003

_____
Dr. Graeme Fairweather
Head Department
Mathematical and Computer Sciences

ABSTRACT

Shadowing is a means of characterizing global errors in the numerical solution of initial value ordinary differential equations by allowing for small perturbations in the initial conditions. The method presented in this thesis allows for estimating a portion of the computed shadowing distance for systems which have a large number of contractive modes. The method is formulated for one-step methods and applied to the Lorenz system, the Chafee-Infante reaction-diffusion equation and a closed-loop thermosyphon.

TABLE OF CONTENTS

LIST OF FIGURES

LIST OF TABLES

ACKNOWLEDGMENTS

I greatly appreciate the help of Dr. Erik Van Vleck, my thesis advisor for his clear explanations, helpful input and patience throughout.

Without the support of the National Science Foundation Grant DMS-9973393, and the Mathematical and Computer Sciences Department at the Colorado School of Mines, this research would not have been possible.

Many thanks go to my thesis committee members, Dr. Paul Martin, Dr. Luis Tenorio and Dr. Graeme Fairweather for their efforts in helping in this process.

Finally, my sincere gratitude goes to my betrothed Monique Deforge and to my family for their support and encouragement.

Chapter 1

INTRODUCTION

Dynamical systems can display sensitive dependence on initial conditions. If, at any point on the solution curve, small changes in the conditions are introduced, this can produce solutions which exponentially diverge from each other a short time later, leading to entirely different solutions. Given the nature of numerical computing, with roundoff errors and discretization errors, we consider the effects these errors, seen as small perturbations, will have on the long-time solution of a system of ODEs. Of particular interest (and of practical importance) is the global error associated with the final time solution of a dynamical system. Does the computed solution suitably represent the exact solution trajectory of the problem being solved?

When categorizing global error, there are at least three methods of error analysis: forward, backward and shadowing. Forward error analysis treats the error equation as an initial value problem (IVP) and the global error may become large over long time intervals unless the problem is contracting. Backward error analysis asks that the computed solution be the solution to a nearby problem and considers a slightly perturbed problem with the same initial conditions. This idea is related to the concept of modified equations [19] and it is not always clear that changing the equation is the best way to go about obtaining the global error estimate. The third type of error analysis, the type with which we concern ourselves, is shadowing. Global error analysis using a shadowing lemma approach involves treating the error equation as a two-point boundary value problem (BVP) as opposed to an IVP. This allows for

shadowing type error analysis results for problems with expansive and contractive directions. Shadowing error analysis involves showing that there exists an exact solution to the differential equation close to the computed solution but with a slightly perturbed initial condition. If one is willing to allow for slight perturbations in the initial conditions, then shadowing can be of great use.

Our main contributions in this thesis are 1) to develop an efficient global error estimate in which the cost of computing the global error estimate is proportional to the number of non-contracting modes in the system of DEs and 2) to produce shadowing results for PDEs which, when discretized to first order ODEs are not always Lipschitz continuous: we consider one-sided Lipschitz constants as an alternative approach. In particular for high dimensional systems, estimating the error in this manner can significantly reduce the cost of global error estimation. We develop a method to produce low-cost shadowing global error estimation for high dimensional systems and show that the global error estimate is proportional to the number of non-contracting modes in a given system. We assume that the systems with which we are working are integrally separated and have bounded growth. These assumptions allow us to use a suitable approximation to the linearization of the system. With this approximation, we use ideas similar in spirit to the recursive projection method [37] and inertial manifold theory [10] to separate our system into two systems: strongly contractive and the rest.

We will reformulate the original differential equation in terms of a new coordinate system that corresponds to the directions associated with the Lyapunov exponents of the linearized problem. We denote the new coordinate system by the columns of an orthogonal matrix function $Q = Q(t)$. This reformulation will allow us to deal with the modes of the system individually, and using our integral separation assumptions

we will show that we can estimate bounds for the contracting modes of the system. Our computations are thus focused on the reduced dimensional systems comprising of those modes which are not strongly contractive, and therefore our global error estimate will be proportional to the number of non-contracting modes in the system.

Our focus numerically is in employing existing IVP solvers and in using Hager style condition number estimation [20, 27] to find the norm of certain matrix pseudo-inverses. The cost is small due to the use of efficient numerical algebra techniques. We will test our hypothesis numerically and give numerical examples with the Lorenz equation, a discretized reaction-diffusion PDE (the Chafee-Infante equation), and a thermosyphon model.

This thesis is organized as follows. In Chapter 2, we present a typical global error estimate in the forward sense, but with using one-sided Lipschitz conditions, and in Chapter 3 we give a brief introduction to numerical shadowing. In Chapter 4, we present the shadowing setup that we will employ throughout this thesis, a fixed point result and consider a reformulation of a linearization of the differential equation by writing the solution $X(t) = Q(t)R(t)$, where $Q(t)$ is a square orthogonal matrix, and by solving for Q and R instead of X. We also state our integral separation and bounded growth assumptions therein. Chapter 5 gives the main theorem and the main result of this thesis. In Chapter 6, we give numerical implementation details; we present our numerical algorithm and detail how we estimate certain values that we will use to obtain a shadowing estimate. Chapter 7 gives numerical examples and Chapter 8 gives our conclusions.

Chapter 2

A BRIEF REVIEW OF GLOBAL ERROR ESTIMATION

In this chapter, we give a standard proof of a global error estimate in the forward sense. This is to illustrate what is typically done to obtain global error estimate bounds in the forward sense when solving systems of differential equations numerically. What is atypical here, is our use of one-sided Lipschitz constants in obtaining our bound.

Consider the autonomous IVP where f is a C^2 function,

$$\begin{cases} \dot{x} &= f(x), \\ x(0) &= x_0, \end{cases} \tag{2.1}$$

and $x \equiv x(t) : \mathbb{R} \to \mathbb{R}^N$ for a positive integer N.

Forward error estimates have historically been obtained by using a Lipschitz condition,

$$\|f(x(t)) - f(y(t))\| \leq c\|x(t) - y(t)\|, \quad c \geq 0. \tag{2.2}$$

Estimates obtained in this manner, while useful, can greatly over-estimate the global error, especially when considering a system which is contracting. This over-estimation is a result of the fact that c is positive which will force the error estimate to grow exponentially in forward time. By considering a one-sided Lipschitz condition, we will be better positioned to estimate the error for the particular dynamics of a given

system.

Definition 2.0.1. *The function f:* $\mathbb{R}^n \to \mathbb{R}^n$ *is said to satisfy a one-sided Lipschitz condition on* $\mathbb{R}^n$ *if there exists* $L \in \mathbb{R}$ *such that*

$$(u-v)^T(f(u)-f(v)) \leq L(u-v)^T(u-v) \quad \forall u, v \in \mathbb{R}^n. \tag{2.3}$$

In the study of differential equations it is common to use the solution operator (also called the evolution operator) to represent the solution to (2.1) as a function of the initial condition, x_0. The solution to (2.1), $x(t)$, can be written

$$x(t) = \phi(x_0, t) \tag{2.4}$$

where ϕ is the solution operator with properties

$$\phi(x_0, 0) = x_0$$

and

$$x(t+s) = \phi(x(s), t) = \phi(x(t), s).$$

The solution operator should be thought of as nothing more than a notational convenience for advancing a solution t time units starting from initial condition x_0.

Suppose that we have local error $e_i = \phi(y_{i-1}, h_{i-1}) - y_i$ with estimate

$$\|e_i\| = \|\phi(y_{i-1}, h_{i-1}) - y_i\| \leq C h_{i-1}^{p+1}, \quad i = 1, \ldots, n, \tag{2.5}$$

where y_i is the computed solution at step i, $\phi(y_{i-1}, h_{i-1})$ is the exact solution at t_i starting from t_{i-1} and h_{i-1} is the ith timestep.

Define

$$\begin{aligned} E_i &= \phi(y_i, t_n - t_i) - \phi(y_{i-1}, t_n - t_{i-1}) \\ &= \phi(y_i, t_n - t_i) - \phi(\phi(y_{i-1}, h_{i-1}), t_n - t_i), \end{aligned} \tag{2.6}$$

where $t_n \equiv t_{end}$, and define the global error to be

$$E = \phi(x_0, t_n - t_0) - y_n. \tag{2.7}$$

We now present a theorem on global error estimation which follows closely one presented in Hairer et al. [23] but using one-sided Lipschitz constants instead of standard Lipschitz constants.

Theorem 2.0.1. *Let U be the solution space of (2.1) where $x(t)$ is the exact solution to (2.1). Suppose that $x, t \in U$ and that they satisfy the one-sided Lipschitz condition (2.3). Also, suppose that the local error estimates (2.5) are satisfied. Then the global error (2.7) can be estimated by*

$$\|E\| \leq h^p \frac{C'}{L} \left(e^{L(t_N - t_0)} - 1\right) \tag{2.8}$$

where $h = \max h_i$,

$$C' = \begin{cases} C, & L \geq 0 \\ Ce^{-Lh}, & L < 0 \end{cases} \tag{2.9}$$

and h is small enough for the numerical solution to remain in U.

Proof. Let

$$x(t) = \phi(\phi(y_{i-1}, h_{i-1}), t_n - t_i)$$

and

$$y(t) = \phi(y_i, t_n - t_i).$$

Then, using the one-sided Lipschitz condition, we obtain

$$\begin{aligned} \frac{d}{dt}\|E_i\|^2 &= \frac{d}{dt}\|x(t) - y(t)\|^2 \\ &= 2(x(t) - y(t))^T(f(x(t)) - f(y(t))) \\ &\leq 2L\|x(t) - y(t)\|^2 \\ &= 2L\|E_i\|^2 \end{aligned} \tag{2.10}$$

By Gronwall's Lemma, for any $t \geq 0$, we have

$$\|E_i\|^2 \leq e^{2L(t_n - t_i)}\|\phi(y_{i-1}, h_{i-1}) - y_i\|^2$$

which implies

$$\|E_i\| \leq e^{L(t_n - t_i)}\|e_i\|.$$

Clearly,

$$\|E\| \leq \sum_{i=1}^{N} \|E_i\|$$

which implies

$$\|E\| \leq \sum_{i=1}^{N} e^{L(t_n - t_i)}\|e_i\|$$

Using (2.5) and the fact that $h_{i-1}^{p+1} \leq h^p h_{i-1}$, we have

$$\|E\| \leq h^p C\left(h_0 e^{L(t_n - t_1)} + h_1 e^{L(t_n - t_2)} + \ldots + 1\right).$$

Notice that

$$\sum_{i=1}^{N} h_{i-1} e^{L(t_n - t_i)} \leq \begin{cases} \int_{t_0}^{t_n} e^{L(t_n - t)} dt, & L \geq 0, \\ \int_{t_0}^{t_n} e^{L(t_n - h - t)} dt, & L < 0, \end{cases} \tag{2.11}$$

which upon integrating will yield the desired global error estimate,

$$\|E\| \leq h^p \frac{C'}{L} \left(e^{L(t_n - t_0)} - 1 \right).$$

Note that if $L = 0$ then (2.11) is trivially true and we get the following error bound,

$$\|E\| \leq h^p C \left(t_n - t_0 \right).$$

□

Chapter 3

INTRODUCTION TO NUMERICAL SHADOWING

Global error analysis using a shadowing lemma approach allows for error analysis results for problems with both expansive and contractive directions. Shadowing is used to show that the numerically obtained solution is a good approximation to an exact solution of the original differential equation (the shadowing solution), but with a slightly different initial condition.

To illustrate shadowing, we give a simple, yet effective, example first given in [35]. Consider the initial value problem,

$$\frac{dx}{dt} = -x, \quad 0 \leq t \leq t_{end}, \quad x(0) = 1, \tag{3.1}$$

which we integrate using Euler's method,

$$x_{n+1} = x_n - hx_n = (1-h)x_n := \psi x_n, \quad 0 \leq n \leq \frac{t_{end}}{h}, \quad x_0 = 1. \tag{3.2}$$

Figure 3.1 depicts the exact solution (solid line) and the computed solution (crosses) when $t_{end} = 5$ and $h = .1$. The maximum absolute value of the error $|e_n| := |x(nh) - x_n|$ is 0.019 and occurs at $n = 10$ (i.e., at $t = 1$). Notice that $|e_n|$ does not grow larger as n increases.

The reason why $|e_n|$ does not grow larger can be simply explained, see, e.g., [28].

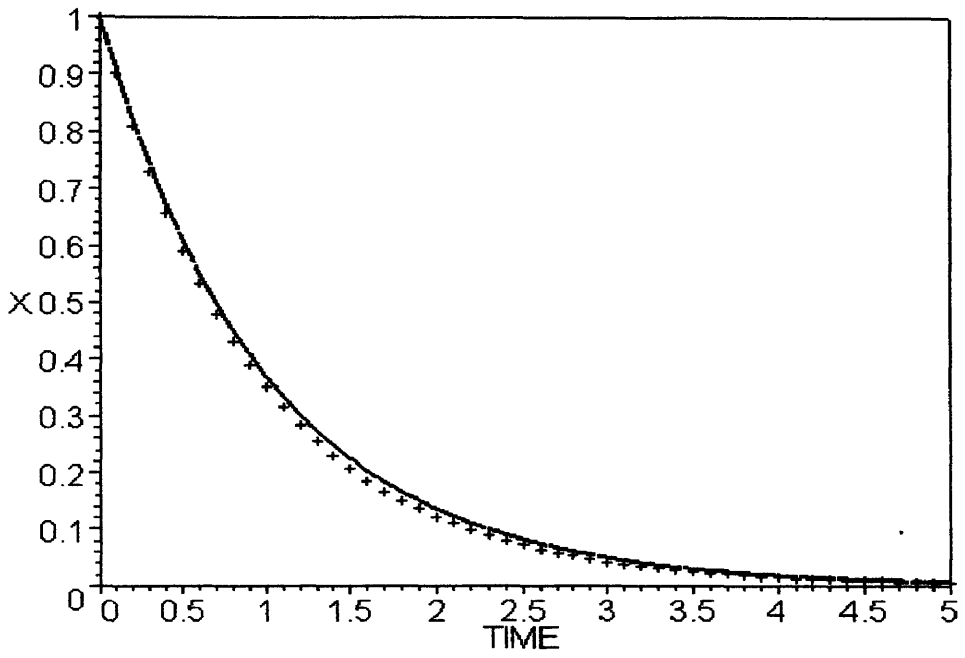

FIG. 3.1. A stable solution trajectory and the exact solution where the numerical errors remain small.

For, we can write

$$\begin{aligned} e_n &= x(nh) - x_n \\ &= x(nh) - \psi x((n-1)h) + \psi x((n-1)h) - \psi x_{n-1}. \end{aligned}$$

Let $l_n = x(nh) - \psi x((n-1)h)$, and we have

$$\begin{aligned} e_n &= \psi x((n-1)h) - \psi x_{n-1} + l_n \\ &= \psi e_{n-1} + l_n. \end{aligned} \tag{3.3}$$

Notice that l_n can be thought of as the local truncation error assocated with each step taken. Since $|\psi| < 1$ for h small enough, there is a dampening in the propagation

of the errors. If we let $l = \sup |l_n|$ and use (3.3), we have

$$\begin{aligned} |e_n| &\leq |\psi||e_{n-1}| + l \\ &\leq |\psi|^2|e_{n-2}| + |\psi|l + l \\ &\leq \ldots \leq \left(\sum_{i=0}^{n-1} |\psi|^i\right) l \leq \frac{l}{h} \end{aligned}$$

using the geometric series and the fact that $e_0 = 0$.

Notice that we have by Taylor's Theorem,

$$\begin{aligned} x(nh) &= x((n-1)h) + h\frac{d}{dt}x((n-1)h) + \frac{1}{2}h^2\frac{d^2x(\xi_n)}{dt^2} \\ &= x((n-1)h) - hx((n-1)h) + \frac{1}{2}h^2\frac{d^2x(\xi_n)}{dt^2}, \quad \xi_n \in ((n-1)h, nh), \end{aligned}$$

that is,

$$l_n = \frac{1}{2}h^2\frac{d^2x(\xi_n)}{dt^2}.$$

Note that

$$\left|\frac{d^2x(t)}{dt^2}\right| = |x(0)e^{-t}| \leq |x(0)|$$

so that for (3.1), $|l_n|$ can be bounded, independently of n, by $\frac{1}{2}h^2|x(0)|$, which yields global error bound,

$$|e_n| \leq \frac{1}{2}h|x(0)|. \tag{3.4}$$

For this problem, $\frac{1}{2}h|x(0)| = .050$ and the maximum actual error is .019.

Now consider an unstable problem,

$$\frac{dx}{dt} = x, \quad 0 \leq t \leq t_{end}, \quad x(0) = 1, \tag{3.5}$$

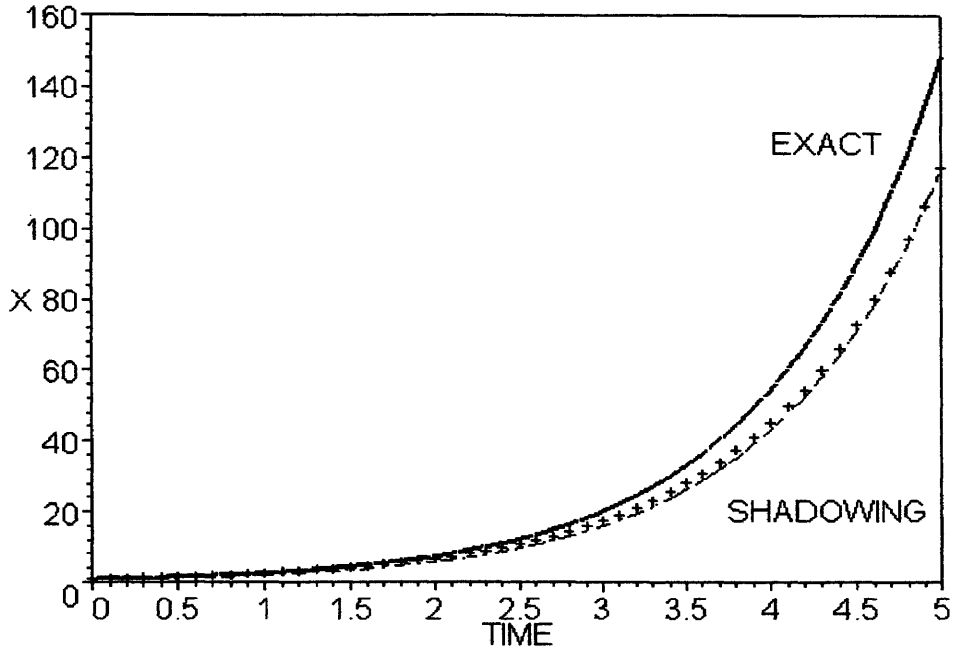

FIG. 3.2. An unstable solution trajectory where the numerical errors grow with time. The numerical solution is a good approximation of the shadowing trajectory.

integrated with Euler's method. Figure 3.2 shows the exact trajectory (solid line) and computed points (crosses). As in Figure 3.1, $t_{end} = 5$ and $h = .1$. Here, the errors grow monotonically as n grows. The largest error 31.0 occurs at t_{end} where $x(5) = 148.4$ and $x_{50} = 117.4$. This is an error of 21%, which is explained by the fact that the errors still satisfy the error recursion (3.3), but $\psi = 1 + h$, leading to exponential growth with n.

If we are willing to allow for different initial conditions, shadowing gives us a means to put to good use the bad numerical results in Figure 3.2 by giving a vastly better global error estimate. Consider the solution $\tilde{x}$ of $dx/dt = x$ that at $t = t_{end}$ has the same value of the numerical solution $x_{50} = 117.4$. The graph of $\tilde{x}$ is given by the dashed line in Figure 3.2 where the initial condition has been found to be $\tilde{x}_0 = 0.79$. The graphs of $\tilde{x}$ and the computed points x_n match much more closely

with the maximum error $|\tilde{x}(nh) - x_n| = 2.07$. This is clearly much better than the error of 31.0 we got from $|x(nh) - x_n|$. It is said that the trajectory $\tilde{x}(t)$ shadows the numerical solution with an accuracy of 2.07.

The result of this example is that the computed points x_n are poor approximations of the solution of (3.5), the problem we integrated numerically. However, they are a good approximation to the shadowing solution: a solution of the same differential equation, but with slightly different initial conditions. If we allow for error in the initial condition, we can produce good global error estimates for problems where we could not previously.

Chapter 4

BACKGROUND AND SETUP

4.1 Shadowing Setup

Before we can give our shadowing theorem, we need to define our error equation and an approximation to the linearization of our error equation which we will use in a fixed-point theorem used to show the existence of a nearby shadowing solution.

Working with the system defined in (2.1), we assume that a numerical solution $y \equiv \{y_k\}_{k=0}^{M}$ using time steps $h \equiv \{h_k\}_{k=0}^{M-1}$, for a positive integer M, has been produced and let $t_{k+1} = t_k + h_k$ with $t_0 = 0$. Consider the operator $G(y,h)$, which is nonlinear in time, with kth block component given by

$$(G(y,h))_k = y_{k+1} - \phi(y_k, h_k) =: \delta_{k+1}, \tag{4.1}$$

for $k = 0, ..., M-1$, where ϕ is the local solution operator as defined in (2.4) and δ_{k+1} is the local error at the kth step. The linearization of $G(y,h)$ is given by

$$(DG(y,h)(\Delta y, \Delta h))_k = \Delta y_{k+1} - D_{y_k}\phi(y_k, h_k)\Delta y_k - \theta D_{h_k}\phi(y_k, h_k)\Delta h_k, \tag{4.2}$$

for $k = 0, ..., M-1$, where $\theta \geq 0$ is a scaling factor [40] and

$$D_{y_k}\phi(y_k, h_k) \equiv \frac{\partial \phi}{\partial y_k}(y_k, h_k)$$

and

$$D_{h_k}\phi(y_k, h_k) \equiv \frac{\partial \phi}{\partial h_k}(y_k, h_k).$$

We assume that $DG(x,h)$ is approximated by a linear operator,

$$(L(\Delta y, \Delta h))_k = \Delta y_{k+1} - Y_k \Delta y_k - \theta f_{k+1} \Delta h_k, \tag{4.3}$$

for $k = 0, ..., M-1$ where $f_{k+1} = f(y_{k+1})$.

We consider $z = y \in \mathbb{R}^{(M+1)N}$ for $\theta = 0$ and $z = (y,h) \in \mathbb{R}^{(M+1)N} \times \mathbb{R}^M$ for $\theta > 0$.

4.2 Fixed Point Result

The following is a fixed point result that has been used in many instances to show the existence of a nearby solution in a shadowing context.

Theorem 4.2.1. *Suppose $\mathcal{X}, \mathcal{Y}$ are Banach spaces, $G : \mathcal{X} \to \mathcal{Y}$ is C^1, and that there exists positive constants ϵ_0, $\alpha < 1$, a point $z \in \mathcal{X}$, and a linear operator $L : \mathcal{X} \to \mathcal{Y}$ with right inverse $L^\dagger$ such that*

$$\|L^\dagger(DG(w) - L)\| \leq \alpha \quad \text{for} \quad \|w - z\| \leq \epsilon_0. \tag{4.4}$$

If, for $0 < \epsilon \leq \epsilon_0$,

$$\|L^\dagger G(z)\| \leq (1-\alpha)\epsilon \tag{4.5}$$

then the equation $G(w) = 0$ has a solution with

$$\|w - z\| \leq \epsilon. \tag{4.6}$$

Our goal now is to find a bound $\alpha < 1$ in (4.4) and a bound on β in (4.5) so that we can set $\epsilon = \beta/(1-\alpha)$ provided $\epsilon \leq \epsilon_0$.

Define the linear variational equation of (2.1) to be the matrix differential equation

$$\dot{X} = Df(x)X \tag{4.7}$$

where $X(t) \in \mathbb{R}^{n \times n}$ is called the fundamental matrix solution of (4.7).

If we write the solution to the linear variational equation as $X(t) = Q(t)R(t)$ (see [13]), where $Q(t)$ is orthogonal and $R(t)$ is upper triangular, then $Q(t)$ satisfies the following matrix differential equation where $S(Q) \equiv S(Q, A(t))$ is a skew-symmetric matrix and $A(t) \equiv Df(x(t))$,

$$\dot{Q} = \left[I - QQ^T\right] AQ + QS(Q) \quad \text{with} \quad S(Q)_{ij} = \begin{cases} (Q^T AQ)_{ij}, & i > j, \\ 0, & i = j, \\ -(Q^T AQ)_{ji}, & i < j, \end{cases} \tag{4.8}$$

and

$$\dot{R} = \tilde{A}R \quad \text{with} \quad \tilde{A} = Q^T AQ - S(Q). \tag{4.9}$$

Clearly the matrix $\tilde{A}(t)$ is upper triangular. We assume that R is of the form,

$$R = \begin{pmatrix} R^{(11)} & R^{(12)} \\ 0 & R^{(22)} \end{pmatrix}$$

where $R^{(11)}$ is a $p \times p$ upper triangular matrix function and $R^{(22)}$ is a $(N-p) \times (N-p)$ upper triangular matrix function.

We solve (4.8) numerically to produce the sequence $\{Q_k\}_{k=0}^{M}$. Simultaneously,

for $k = 0, ..., M-1$, we solve

$$\begin{cases} \dot{\tilde{R}}_k(t) = & \tilde{A}(t+t_k)\tilde{R}_k(t), \\ \tilde{R}_k(0) = & I, \end{cases} \tag{4.10}$$

for $0 \leq t \leq h_k$ and let R_k denote the approximation to $\tilde{R}(h_k)$.

4.3 Background on Integral Separation

We make the assumption in this thesis that the fundamental matrix solution of the linear variational equation with which we are working is integrally separated. This implies certain things about the columns of the fundamental matrix solution as well as the elements on the diagonal of the matrix $\tilde{A}$. Most importantly, this implies that the functions on the diagonal of the matrix $\tilde{A}$ are integrally separated. We present a definition of integral separation for fundamental matrix solutions first found in Adrianova [1] and later presented in [14].

Definition 4.3.1. *[1, Property 5.3.2], [14] Write a fundamental matrix solution columnwise* $X(t) = [X_1(t), ..., X_n(t)]$. *Then* X *is integrally separated if for* $i = 1, ..., n-1$, *there exist positive constants* a *and* d *such that*

$$\frac{\|X_i(t)\|}{\|X_i(s)\|} \cdot \frac{\|X_{i+1}(s)\|}{\|X_{i+1}(t)\|} \geq de^{a(t-s)}, \tag{4.11}$$

for all t, s *such that* $t \geq s$.

In particular if we have a system in which the fundamental matrix solution is integrally separated then the system has distinct Lyapunov exponents. Also, integral separation is kept under certain transformations such as our $X = QR$.

We present another definition of integral separation for functions.

Definition 4.3.2. *The functions g_i, $i = 1, ..., n$, are said to be integrally separated if for $i = 1, ..., n-1$,*

$$\int_s^t [g_i(\tau) - g_{i+1}(\tau)]\, d\tau \geq a(t-s) - d, \quad t \geq s, \quad a > 0 \in \mathbb{R}, \quad d \in \mathbb{R}. \tag{4.12}$$

The integral separation assumption for functions is something which will allow us to verify that the elements on the diagonal of $\tilde{A}$ are in fact integrally separated.

4.4 Assumptions Based on Integral Separation and Bounded Growth

We solve (4.10) numerically to produce a sequence $\{R_k\}_{k=0}^{M-1}$. We assume, for this sequence, that there exists positive constants $K, J \geq 1$, $0 < d \leq 1$, $a, \omega > 0$, and $\gamma \in \mathbb{R}$ such that

$$\|R_j^{(11)} \cdots R_k^{(11)}\|_\infty \leq K e^{\gamma(t_{j+1} - t_k)}, \quad j \geq k, \tag{4.13}$$

$$\|(R_j^{(11)} \cdots R_k^{(11)})^{-1}\|_\infty \cdot \|R_j^{(22)} \cdots R_k^{(22)}\|_\infty \leq \frac{1}{d} e^{-a(t_{j+1} - t_k)}, \quad j \geq k, \tag{4.14}$$

and

$$\|R_j^{(22)} \cdots R_k^{(22)}\|_\infty \leq J e^{\omega(t_{j+1} - t_k)}, \quad j \geq k. \tag{4.15}$$

The first assumption (4.13) is that there is bounded growth in the linearized equation (see [11]), the second assumption (4.14) is that there is integral separation (see [1]) between the $(1,1)$ and $(2,2)$ blocks, while the third assumption (4.15) states that the $(2,2)$ block is contracting. We approximately verify these assumptions in practice by using constructions motivated by Steklov function considerations. For a discussion on testing integral separation see [14].

4.5 Decomposition of the Linearized Operator and the Pseudo Inverse

We choose for the right inverse, $L^\dagger$, in Theorem (4.2.1), the pseudo inverse. This allows us to find $L^\dagger$ explicitly which is useful when determining the bounds for α and β in (4.4) and (4.5). The choice of the pseudo inverse also has the advantage that it is independent of the dynamics of the problem, i.e., it does not depend on the number of stable, unstable, or neutral modes and it is the optimal choice with respect to the 2-norm.

When solving (4.8) for $Q(t)$ we will only solve for the first p columns of $Q(t)$ where p is the number of non-contracting modes in the original IVP, (2.1). We will then complete Q with the orthogonal complement to the first p columns. Thus, Q will be of the form $Q = [\tilde{Q}|\tilde{Q}^\perp]$ where $\tilde{Q} \in \mathbb{R}^{N\times p}$ and $\tilde{Q}^\perp \in \mathbb{R}^{N\times(N-p)}$.

If we obtain R_k from (4.9), then in (4.3) we have $Y_k = Q_{k+1}R_kQ_k^T$. The linear operator L in (4.3) can be written as $L = \overline{Q}U\hat{Q}^T$, where $\overline{Q}, \hat{Q}$ are block diagonal matrices given by

$$\overline{Q} = \text{diag}(Q_1, ..., Q_M),\ \hat{Q} = \text{diag}(Q_0, ..., Q_M, I_M), \tag{4.16}$$

where I_M is the $M \times M$ identity matrix. The matrix U is given, in block indices, by

$$(U(z,\tau))_k = z_{k+1} - R_kz_k - \theta g_{k+1}\tau_k \tag{4.17}$$

where $f_{k+1} = Q_{k+1}g_{k+1}$.

Using the assumptions based on integral separation and bounded growth, we approximate L with $\tilde{L}$ where

$$\tilde{L} = \bar{Q}D\hat{Q}^T, \quad (D(z,\tau))_k = z_{k+1} - \hat{R}_kz_k - \theta g_{k+1}\tau_k \tag{4.18}$$

and

$$\hat{R}_k = \begin{pmatrix} R_k^{(11)} & 0 \\ 0 & R_k^{(22)} \end{pmatrix}.$$

Thus, the pseudo inverse of $\tilde{L}$, $\tilde{L}^\dagger$, can be written as

$$\tilde{L}^\dagger = \hat{Q} D^\dagger \overline{Q}^T, \tag{4.19}$$

where $D^\dagger$ is the pseudo inverse of D.

We write $D^\dagger = D^T(DD^T)^{-1}$ and note that DD^T is symmetric and block tridiagonal with entries $(DD^T)_{k,k} = I + \hat{R}_k \hat{R}_k^T + \theta^2 g_{k+1} g_{k+1}^T$ for $k = 0, ..., M-1$ and $(DD^T)_{k-1,k} = -\hat{R}_k^T$ for $k = 1, ..., M-1$.

Using our assumptions based on integral separation, we will break the bound for $D^\dagger$ into two estimates and let the bound be the greater of the two. We will estimate a value for the rows corresponding to contracting modes and solve a linear system to obtain the bound for the non-contracting modes.

When solving for the pseudoinverse of D, $D^\dagger$, we notice that there are two disjoint systems involved, corresponding to the contracting and non-contracting modes of this equation. In order to obtain the supremum norm in as efficient a manner as possible we will separate $D^\dagger$ into two systems corresponding to the different modes, take the sup norm of each system and take the greater of these two as our norm.

Let $A = DD^T$. The matrix A is block tridiagonal. To form $D^\dagger$ we can solve the equation $A(D^\dagger)^T = D$ since $D^\dagger = D^T(DD^T)^{-1}$. This method is unnecessarily slow when there are contracting modes for the system.

Given that DD^T is block tridiagonal and D is block bidiagonal, we observe that

$(D^\dagger)^T$ will have the form:

$$(D^\dagger)^T = \begin{pmatrix} (D^\dagger)^T_{1,1} & 0 & (D^\dagger)^T_{1,3} & 0 & \cdots \\ 0 & (D^\dagger)^T_{2,2} & 0 & (D^\dagger)^T_{2,4} & \\ (D^\dagger)^T_{3,1} & 0 & (D^\dagger)^T_{3,3} & 0 & \\ \vdots & & & & \ddots \end{pmatrix}. \tag{4.20}$$

This alternating block form allows us to separate this system into two systems $(D_1 D_1^T)(D_1^\dagger)^T = D_1$ and $(D_2 D_2^T)(D_2^\dagger)^T = D_2$ where we define

$$D_i = \left(\begin{array}{cccc|ccc} -R_0^{(ii)} & I & & & -\theta g_1^{(i)} & & \\ & \ddots & \ddots & & & \ddots & \\ & & -R_M^{(ii)} & I & & & -\theta g_{M+1}^{(i)} \end{array}\right)$$

for $i = 1, 2$,

$$(D_1^\dagger)^T = \begin{pmatrix} (D^\dagger)^T_{1,1} & \cdots & (D^\dagger)^T_{1,2M+1} \\ \vdots & \ddots & \\ (D^\dagger)^T_{2M-1,1} & & \end{pmatrix}$$

and

$$(D_2^\dagger)^T = \begin{pmatrix} (D^\dagger)^T_{2,2} & \cdots & (D^\dagger)^T_{2,2M+2} \\ \vdots & \ddots & \\ (D^\dagger)^T_{2M,2} & & \end{pmatrix}.$$

The $(D_1^\dagger)^T$ system will correspond to the non-contracting modes of D while the $(D_2^\dagger)^T$ system will correspond to the contracting modes of D.

Chapter 5

MAIN THEOREM

Our main theorem is a statement of a shadowing type global error result for potentially high dimensional initial value ODEs with a large number of contracting modes. The main advantage over previous results is that the work required to find the global error bound is proportional to the number of expanding modes. The idea behind the theorem is to bound α and β in Theorem 4.2.1. We found it useful to apply Theorem 4.2.1 with a norm based upon the orthogonal matrices $\{Q_k\}_{k=0}^{M}$. Much of the technical difficulty in the proof is due to the fact that we only assume that the first p columns for some $p < N$ of each Q_k are known.

We will apply Theorem 4.2.1 in the norm $\|x\|_{\hat{Q}^T,\infty} = \|\hat{Q}^T x\|_\infty$ where $\hat{Q}$ is defined in (4.16). This vector norm, as the following lemma shows, induces the matrix norm $\|A\|_{\hat{Q}^T,\hat{Q},\infty} = \|\hat{Q}^T A\hat{Q}\|_\infty$ for appropriately sized square matrices.

Lemma 5.1.1. *The vector norm*

$$\|x\|_{\hat{Q}^T,\infty} = \|\hat{Q}^T x\|_\infty$$

induces the matrix norm

$$\|A\|_{\hat{Q}^T,\hat{Q},\infty} = \|\hat{Q}^T A\hat{Q}\|_\infty.$$

Proof. Consider $\|y\|_{\hat{Q}^T,\infty} = \|\hat{Q}^T y\|_\infty$

Then

$$\begin{aligned}\sup_{\|y\|_{\hat{Q}^T,\infty}=1} \|Ay\|_{\hat{Q}^T,\infty} &= \sup_{\|\hat{Q}^T y\|_\infty=1} \|\hat{Q}^T A y\|_\infty \\ &= \sup_{\|x\|_\infty=1} \|\hat{Q}^T A \hat{Q} x\|_\infty \\ &= \|\hat{Q}^T A \hat{Q}\|_\infty. \end{aligned} \tag{5.1}$$

□

With these norms, we now state a shadowing theorem for initial value ODEs.

Theorem 5.1.1. *Consider an approximate solution $\{x_k\}_{k=0}^M$, with timesteps $\{h_k\}_{k=0}^{M-1}$ to the IVP (2.1). Let $\theta \geq 0$ be given and consider G given by (4.1), DG given by (4.2) and L as in (4.3). Assume that, for $k = 0, ..., M-1$, we have $\|(G(x,h))_k\|_2 \leq \delta$ for some $\delta > 0$ and assume that (4.13) - (4.15) hold.*

For $\epsilon_0 > 0$, consider $\tilde{L}$ given in (4.18) and $\bar{Q}$ and $\hat{Q}$ given in (4.16). Let

$$\|\bar{Q}^T(DG(w) - DG(z))\hat{Q}\|_\infty \leq \alpha_1$$

for all w such $\|\hat{Q}^T(w-z)\|_\infty \leq \epsilon_0$,

$$\|\bar{Q}^T(DG(z) - L))\hat{Q}\|_\infty \leq \alpha_2$$

and

$$\|U - D\|_\infty \leq \alpha_3.$$

Define $\alpha = \eta\,(\alpha_1 + \alpha_2 + \alpha_3)$, where $\|D^\dagger\|_\infty \leq \eta$ and $\eta = \max\{\eta_1, \eta_2\}$ with $\|D_1^\dagger\|_\infty \leq$

η_1 *and*

$$\|D_2^\dagger\|_\infty \leq \eta_2 := J\left[e^{\omega(t_M - t_1)} + ... + e^{\omega(t_M - t_{M-2})} + e^{\omega(t_M - t_{M-1})}\right] + 1.$$

If $\alpha < 1$, *then define* $\beta = \eta\delta$ *and set* $\epsilon = \frac{\beta}{1-\alpha}$. *If* $\epsilon \leq \epsilon_0$, *then there exists* $\{y_k\}_{k=0}^M$ *and* $\{\tau_k\}_{k=0}^{M-1}$ *such that* $y_{k+1} = \phi(y_k, \tau_k)$ *for* $k = 0, 1, ..., M-1$ *(i.e.* $\{y_k\}_{k=0}^M$ *and* $\{\tau_k\}_{k=0}^{M-1}$ *defines an exact solution to the differential equation as* $y_k = x(t_k)$ *for all* t_k*),* *and* $\|Q_k^T(x_k - y_k)\|_\infty \leq \epsilon$ *for* $k = 0, 1, ..., M$ *and* $|h_k - \tau_k| \leq \theta\epsilon$, *for* $k = 0, 1, ..., M-1$.

Before proving the theorem, we state some lemmas we will need for the proof. The lemmas will provide bounds for the terms α_1, α_2, and α_3 in Theorem 5.1.1 that contribute to bounding α in Theorem 4.2.1.

We decompose $\tilde{L}^\dagger$ as in (4.19) and, for $\|\hat{Q}^T(w - z)\|_\infty \leq \epsilon_0$, write

$$\begin{aligned}
\|\tilde{L}^\dagger(DG(w) - \tilde{L})\|_{\hat{Q}^T,\hat{Q},\infty} &= \|\hat{Q}D^\dagger\bar{Q}^T(DG(w) - \tilde{L})\|_{\hat{Q}^T,\hat{Q},\infty} \\
&= \|D^\dagger\bar{Q}^T(DG(w) - DG(z) + DG(z) - L + L - \tilde{L})\hat{Q}\|_\infty \\
&\leq \|D^\dagger\|_\infty \Big\{ \|\bar{Q}^T(DG(w) - DG(z))\hat{Q}\|_\infty \\
&+ \|\bar{Q}^T(DG(z) - L)\hat{Q}\|_\infty + \|U - D\|_\infty \Big\}. \qquad (5.2)
\end{aligned}$$

To facilitate the derivation of bounds on these terms, we write the differential equation locally as

$$\frac{\partial}{\partial t}\phi(y_k, t) = f(\phi(y_k, t)) \equiv Df(\phi(x_k, t))\phi(y_k, t) + g(\phi(y_k, t)), \qquad (5.3)$$

where $g(\phi(y_k, t)) = f(\phi(y_k, t)) - Df(\phi(x_k, t))\phi(y_k, t)$. We write the local solution

using the nonlinear variation of constants as

$$\phi(y_k,t) = \Phi(t,0)y_k + \int_0^t \Phi(t,s)g(\phi(y_k,s))ds \tag{5.4}$$

where $\Phi(t,0)$ is the principal matrix solution to the linear variational equations

$$\dot{\Phi}(t,0) = Df(\phi(x_k,t))\Phi(t,0),\ \Phi(0,0) = I. \tag{5.5}$$

Lemma 5.1.2. *Assume that $\epsilon_0 > 0$ is given and that there exists real constants $M^{(k)}, L_{f,2}^{(k)}, L_{f,3}^{(k)}$ and $B_{g_x}^{(k)}$ for $k = 0,\ldots,M$ such that the following Lipschitz conditions are satisfied*

$$\|\frac{\partial^2}{\partial x_k \partial \phi} g(\phi(x_k,t))\|_\infty \leq M^{(k)} \tag{5.6}$$

$$(\phi(x_k,t) - \phi(y_k,t))^T (f(\phi(x_k,t)) - f(\phi(y_k,t))) \leq L_{f,2}^{(k)} \|\phi(x_k,t) - \phi(y_k,t)\|_2^2 \tag{5.7}$$

$$\begin{aligned}&(f(\phi(x_k,t)) - f(\phi(y_k,t)))^T (Df(\phi(x_k,t))f(\phi(x_k,t)) - Df(\phi(y_k,t))f(\phi(y_k,t))) \\ &\leq L_{f,3}^{(k)} \|f(\phi(x_k,t)) - f(\phi(y_k,t))\|_2^2\end{aligned} \tag{5.8}$$

$$\|\frac{\partial}{\partial x_k} f(\phi(x_k,t))\|_\infty \leq B_{g_x}^{(k)} \tag{5.9}$$

for $\|Q_k^T(x_k - y_k)\|_\infty \leq \epsilon_0$ in an appropriate neighborhood of the local solution $\phi(x_k,t)$.

Then

$$\|\phi(x_k,t) - \phi(y_k,t)\|_2 \leq \|x_k - y_k\|_2 \, e^{L_{f,2}^{(k)} t}\ , \tag{5.10}$$

$$\|f(\phi(x_k,t)) - f(\phi(y_k,t))\|_2 \leq \|f(x_k) - f(y_k)\|_2 \, e^{L_{f,3}^{(k)} t}\ , \tag{5.11}$$

and

$$\|Q_{k+1}^T(\phi_{x_k}(x_k,t)-\phi_{y_k}(y_k,t))Q_k\|_\infty \leq KM^{(k)}\|x_k-y_k\|_2\, e^{\gamma t}\int_0^t e^{(L_{f,2}^{(k)}-\gamma)s}ds. \quad (5.12)$$

Proof. We have

$$\begin{aligned} & (\phi(x_k,t)-\phi(y_k,t))^T(f(\phi(x_k,t))-f(\phi(y_k,t))) \\ \leq\ & L_{f,2}^{(k)}\|\phi(x_k,t)-\phi(y_k,t)\|_2^2 \end{aligned}$$

to which we apply Gronwall's Lemma, yielding,

$$\|\phi(x_k,t)-\phi(y_k,t)\|_2 \ \leq\ \|x_k-y_k\|_2\, e^{L_{f,2}^{(k)}t}.$$

Also, in a similar manner, after applying Gronwall's Lemma we obtain

$$\|f(\phi(x_k,t))-f(\phi(y_k,t))\|_2 \leq \|f(x_k)-f(y_k)\|_2\, e^{L_{f,3}^{(k)}t}$$

and if we use the fact that $\phi(x,0)=x$, the result (5.11) is obtained.

Finally, we write

$$\phi_{x_k}(x_k,t)=\Phi(t,0)+\int_0^t \Phi(t,s)\frac{\partial}{\partial x_k}g(\phi(x_k,s))ds. \quad (5.13)$$

This implies

$$\begin{aligned}
& \|Q_{k+1}^T(\phi_{x_k}(x_k,t)-\phi_{y_k}(y_k,t))Q_k\|_\infty \\
\leq & \int_0^t \|\Phi(t,s)\|_\infty \|\frac{\partial}{\partial x_k}g(\phi(x_k,s))-\frac{\partial}{\partial y_k}g(\phi(y_k,s))\|_\infty ds \\
\leq & \int_0^t Ke^{\gamma(t-s)}\| \int_0^1 \frac{\partial^2}{\partial x \partial \phi}g(\phi(y_k,s)-\theta[\phi(x_k,s) \\
- & \phi(y_k,s)])d\theta\,(\phi(x_k,s)-\phi(y_k,s))\,\|_\infty ds \\
\leq & \int_0^t Ke^{\gamma(t-s)} \int_0^1 M^{(k)}d\theta \|x_k-y_k\|_2\, e^{L_{f,2}^{(k)}s}ds \\
= & KM^{(k)}\|x_k-y_k\|_2\, e^{\gamma t}\int_0^t e^{(L_{f,2}^{(k)}-\gamma)s}ds. \qquad (5.14)
\end{aligned}$$

□

Lemma 5.1.3. *Given $\epsilon_0 > 0$ and $\theta \geq 0$. Then, for $|h_k - \tau_k| \leq \theta\epsilon_0$ and $\|Q_k^T(x_k - y_k)\|_\infty \leq \epsilon_0$,*

$$\begin{aligned}
& \|f(\phi(x_k,h_k))-f(\phi(y_k,\tau_k))\|_2 \\
\leq & \|f(\phi(x_k,\theta\epsilon_0))-f(\phi(y_k,\tau_k-h_k+\theta\epsilon_0))\|_2\, e^{L_{f,3}^{(k)}(h_k-\epsilon_0\theta)}. \qquad (5.15)
\end{aligned}$$

Proof. Applying Gronwall's Lemma to our Lipschitz condition (5.8) yields

$$\begin{aligned}
& \|f(\phi(x_k,h_k))-f(\phi(y_k,\tau_k))\|_2 \\
\leq & \|f(\phi(x_k,\theta\epsilon_0))-f(\phi(y_k,\tau_k-h_k+\theta\epsilon_0))\|_2\, e^{L_{f,3}^{(k)}(h_k-\epsilon_0\theta)}.
\end{aligned}$$

□

We consider next a bound on the term $\|\bar{Q}^T(DG(z)-L)\hat{Q}\|_\infty$ of (5.2).

Lemma 5.1.4. *If the local error in approximating the solution to the linear variational equation is $C_1\delta$ where δ is a uniform bound on the local error of the differential*

equation (2.1), then

$$\|\bar{Q}^T(DG(z) - L)\hat{Q}\|_\infty \leq \alpha_1$$

where

$$\alpha_1 = C_1\delta + \theta \max_k \|f(z_k) - f(x_k)\|_2 \, e^{L_{f,3}^{(k)} h_k},$$

where z_k is such that $\phi(z_k, h_k) = x_{k+1}$.

Proof. We have

$$\| \left(\bar{Q}^T(DG(z) - L)\hat{Q}\right)_{kk} \|_\infty \;=\; \|Q_{k+1}^T(\phi_{x_k}(x_k, h_k) - Y_k)Q_k\|_\infty \tag{5.16}$$

which is controlled using local error control. By using (5.8) and the fact that there exists z_k such that $\phi(z_k, h_k) = x_{k+1}$, we have

$$\|Q_{k+1}^T(f(x_{k+1}) - f(\phi(x_k, h_k)))\|_\infty \leq \|f(z_k) - f(x_k)\|_2 \, e^{L_{f,3}^{(k)} h_k}.$$

□

We now consider the term $\|\bar{Q}^T(DG(w) - DG(z))\hat{Q}\|_\infty$ of (5.2) in a similar manner.

Lemma 5.1.5. *Let $\epsilon_0 > 0$ be given. Then for $\|\hat{Q}^T(w - z)\|_\infty \leq \epsilon_0$, $\|\bar{Q}^T(DG(w) - DG(z))\hat{Q}\|_\infty \leq \alpha_2$ where*

$$\begin{aligned}
\alpha_2 \;&=\; \max_k(\theta \|f(\phi(x_k, \theta\epsilon_0)) - f(\phi(y_k, \tau_k - h_k + \theta\epsilon_0))\|_2 \, e^{L_{f,3}^{(k)}(h_k - \epsilon_0\theta)} \\
&+\; KM^{(k)}\|x_k - y_k\|_2 \, e^{\gamma(h_k + \theta\epsilon_0)} \int_0^{h_k + \theta\epsilon_0} e^{(L_{f,2}^{(k)} - \gamma)s} ds \\
&+\; \theta\epsilon_0 \max_{|s - h_k| \leq \theta\epsilon_0} \|Q_{k+1}^T \frac{\partial}{\partial x_k} f(\phi(x_k, s))Q_k\|_\infty.
\end{aligned} \tag{5.17}$$

Proof. The term $\theta\|Q_{k+1}^T(f(\phi(x_k,h_k)) - f(\phi(y_k,\tau_k)))\|_\infty$ is bounded using Lemma 5.1.3. We have

$$\begin{aligned}\| \left(\bar{Q}^T(DG(w) - DG(z))\hat{Q}\right)_{kk} \|_\infty &= \|Q_{k+1}^T(\phi_{x_k}(x_k,h_k) - \phi_{y_k}(y_k,\tau_k))Q_k\|_\infty \\ &= \|Q_{k+1}^T(\phi_{x_k}(x_k,\tau_k) - \phi_{y_k}(y_k,\tau_k))Q_k\|_\infty \\ &+ \|Q_{k+1}^T(\phi_{x_k}(x_k,h_k) - \phi_{x_k}(x_k,\tau_k))Q_k\|_\infty \end{aligned} \tag{5.18}$$

The first term in (5.18) is bounded using (5.7) and Lemma 5.1.2. To bound the second term, we have

$$\begin{aligned}\|Q_{k+1}^T(\phi_{x_k}(x_k,h_k) - \phi_{x_k}(x_k,\tau_k))Q_k\|_\infty &\leq \|Q_{k+1}^T \int_{\tau_k}^{h_k} \frac{\partial}{\partial x_k} f(\phi(x_k,s))ds Q_k\|_\infty \\ &\leq \theta\epsilon_0 \max_{|s-h_k|\leq\theta\epsilon_0} \|Q_{k+1}^T \frac{\partial}{\partial x_k} f(\phi(x_k,s))Q_k\|_\infty. \end{aligned} \tag{5.19}$$

□

Lemma 5.1.6. *Assume that (4.13) and (4.14) hold. Then* $\|U - D\|_\infty \leq \alpha_3$, *where*

$$\alpha_3 = \max_k \{K e^{\gamma(t_{k+1}-t_k)} \frac{M_{\tilde{A}^{(12)}}}{ad} \left[1 - e^{-a(t_{k+1}-t_k)}\right]\} \tag{5.20}$$

and $M_{\tilde{A}^{(12)}}$ *is a uniform bound on the coefficients of the upper triangular matrix function* $\tilde{A}$ *in (4.9) obtained from the coefficient matrix of the linear variational equation (4.7) by the orthogonal change of variables.*

Proof. To bound $\|U - D\|_\infty$, write

$$R(t) = Z(t)D(t) \tag{5.21}$$

where

$$Z(t) = \begin{pmatrix} I & W(t) \\ 0 & I \end{pmatrix}, \quad Z(+\infty) = I. \tag{5.22}$$

By taking the derivative of (5.21) and using (4.10), we obtain the following differential equation for $W(t)$

$$\begin{cases} \dot{W} = & \tilde{A}^{(11)}W - W\tilde{A}^{(22)} + \tilde{A}^{(12)}, \\ W(+\infty) = & 0. \end{cases} \tag{5.23}$$

Solving (5.23) for $W(t)$ yields:

$$W(t) = -R^{(11)}(t)\left[\int_t^{\infty} R^{(11)^{-1}}(s)\tilde{A}^{(12)}(s)R^{(22)}(s)ds\right] R^{(22)^{-1}}(t). \tag{5.24}$$

We define $Z_1 = \text{diag}(Z(t_1), ..., Z(t_M))$ and $Z_2 = \text{diag}(I, Z^{-1}(t_1), ..., Z^{-1}(t_M))$ for timesteps $t_1, ..., t_M$. This allows us to write $U = Z_1 D Z_2$ since

$$R_k = \begin{pmatrix} I & W(t_{k+1}) \\ 0 & I \end{pmatrix} \hat{R}_k \begin{pmatrix} I & -W(t_k) \\ 0 & I \end{pmatrix}, \quad \hat{R}_k = \begin{pmatrix} R_k^{(11)} & 0 \\ 0 & R_k^{(22)} \end{pmatrix}. \tag{5.25}$$

We now use this reformulation to find a bound on $\|U - D\|_\infty = \|Z_1 D Z_2 - D\|_\infty$. For $k = 0, ..., M-1$ we have that the (k,k) block of $U - D$ is

$$(U - D)_{k,k} = \begin{pmatrix} 0 & -R_k^{(11)}W(t_k) + W(t_{k+1})R_k^{(22)} \\ 0 & 0 \end{pmatrix}. \tag{5.26}$$

What remains is to derive a bound on $-R_k^{(11)}W(t_k) + W(t_{k+1})R_k^{(22)}$. We use assump-

tions (4.13) and (4.14). We have

$$
\begin{aligned}
& \| - R_k^{(11)} W(t_k) + W(t_{k+1}) R_k^{(22)} \|_\infty \\
= \; & \| R_k^{(11)} R^{(11)}(t_k) \left[\int_{t_k}^{\infty} R^{(11)^{-1}}(s) \tilde{A}^{(12)}(s) R^{(22)}(s) ds \right] R^{(22)^{-1}}(t_k)] \\
- \; & R^{(11)}(t_{k+1}) \left[\int_{t_{k+1}}^{\infty} R^{(11)^{-1}}(s) \tilde{A}^{(12)}(s) R^{(22)}(s) ds \right] R^{(22)^{-1}}(t_{k+1}) R_k^{(22)} \|_\infty \\
= \; & \| R^{(11)}(t_{k+1}) \left[\int_{t_k}^{t_{k+1}} R^{(11)^{-1}}(s) \tilde{A}^{(12)}(s) R^{(22)}(s) ds \right] R^{(22)^{-1}}(t_k) \|_\infty \\
= \; & \| R_k^{(11)} R^{(11)}(t_k) \left[\int_{t_k}^{t_{k+1}} R^{(11)^{-1}}(s) \tilde{A}^{(12)}(s) R^{(22)}(s) ds \right] R^{(22)^{-1}}(t_k) \|_\infty \\
\leq \; & \| R_k^{(11)} \|_\infty \int_{t_k}^{t_{k+1}} \| R^{(11)}(t_k) R^{(11)^{-1}}(s) \|_\infty \| \tilde{A}^{(12)}(s) \|_\infty \| R^{(22)}(s) R^{(22)^{-1}}(t_k) \|_\infty ds.
\end{aligned}
$$

At this point, we use (4.14) and the bound $M_{\tilde{A}^{(12)}}$ on the elements of $\tilde{A}^{(12)}$. Then

$$
\begin{aligned}
\| U - D \|_\infty &\leq \| R^{(11)}(t_{k+1}) R^{(11)^{-1}}(t_k) \|_\infty \frac{M_{\tilde{A}^{(12)}}}{d} \int_{t_k}^{t_{k+1}} e^{-a(s-t_k)} ds \\
&\leq K e^{\gamma(t_{k+1}-t_k)} \frac{M_{\tilde{A}^{(12)}}}{ad} \left[1 - e^{-a(t_{k+1}-t_k)} \right], \qquad (5.27)
\end{aligned}
$$

where $\| R_k^{(11)} \|$ is bounded using (4.13). □

Proof of Theorem 5.1.1. The idea of the proof is to bound α and β in Theorem 4.2.1 using the norms in Lemma 5.1.1 with the operator L replaced by $\tilde{L}$ (see (4.17) and

(4.18)). For β in (4.5), we have

$$\|\tilde{L}^\dagger G(x)\|_{\hat{Q}^T,\infty} = \|\hat{Q}^T\tilde{L}^\dagger G(x)\|_\infty = \|D^\dagger\bar{Q}^T G(x)\|_\infty \le \|D^\dagger\|_\infty \cdot \|\bar{Q}^T G(x)\|_\infty, \quad (5.28)$$

and $\|D^\dagger\|_\infty \le \eta$. To obtain a bound on $\|\bar{Q}^T G(x)\|_\infty$, we have,

$$\|\bar{Q}^T G(x)\|_\infty = \sup_k \|Q_k^T\delta_k\|_\infty = \sup_k \sup_i |(Q_k^T\delta_k)_i| \le \sup_k \|\delta_k\|_2 = \delta, \quad (5.29)$$

using the Cauchy-Schwarz inequality since local error is bounded by δ in the Euclidean norm. Thus, we have $\|\tilde{L}^\dagger G(x)\|_{\hat{Q}^T,\infty} \le \eta\delta =: \beta$.

Next decompose $\tilde{L}^\dagger$ as in (4.19) and, for $\|\hat{Q}^T(w-z)\|_\infty \le \epsilon_0$, we have by (5.2) that

$$\begin{aligned} \|\tilde{L}^\dagger(DG(w)-\tilde{L})\|_{\hat{Q}^T,\hat{Q},\infty} &\le \|D^\dagger\|_\infty \Big\{ \|\bar{Q}^T(DG(w)-DG(z))\hat{Q}\|_\infty \\ &+ \|\bar{Q}^T(DG(z)-L)\hat{Q}\|_\infty + \|(U-D)\|_\infty \Big\} \quad (5.30) \\ &\le \eta\cdot(\alpha_2+\alpha_1+\alpha_3) =: \alpha, \quad (5.31) \end{aligned}$$

where α_1, α_2, and α_3 are bounded in Lemmas 5.1.4, 5.1.5, and 5.1.6, respectively.

Finally to bound $\|D_2^\dagger\|_\infty$ by η_2, we consider the solution to $D_2 z = g$ for $\|g\|_\infty < 1$ and use (4.15). We have

$$\begin{cases} z_{k+1}^{(2)} = R_k^{(22)} z_k^{(2)} + g_k, \\ z_0^{(2)} = 0. \end{cases} \quad (5.32)$$

For $k \ge l$ define $\Phi_{k,l} = \prod_{j=l}^k R_j^{(22)}$. Then $z_{k+1}^{(2)} = \Phi_{k,0} z_0^{(2)} + \Phi_{k,1} g_0 + \ldots + \Phi_{k,k-1} g_{k-2} + \Phi_{k,k} g_{k-1} + g_k$. Thus,

$$\|z_{k+1}\|_\infty \le J\left[e^{\omega(t_{k+1}-t_1)} + \ldots + e^{\omega(t_{k+1}-t_{k-1})} + e^{\omega(t_{k+1}-t_k)}\right] + 1, \quad (5.33)$$

and η_2 is set to the bound obtained in (5.33) with $k+1 = M$.

This completes the proof. $\square$

Chapter 6

IMPLEMENTATION

The basic outline of our algorithm for solving and producing a shadowing distance estimate for an approximate solution of the IVP (2.1) follows.

6.1 Algorithm

Given constant $\epsilon_0 > 0$:

1. Simultaneously approximate solutions to (4.8) and (4.9).

2. Find bounds for the quantities $\overline{Q}^T(DG(w)-DG(z))\hat{Q}$, $U-D$ and $\overline{Q}^T(DF(w)-L)\hat{Q}$ using Lemmas (5.1.4), (5.1.5) and (5.1.6).

3. Estimate $\|D^\dagger\|_\infty$ using Hager's algorithm and (5.33).

4. Using the results from Steps 2 and 3, estimate α in (4.4) and β in (4.5).

5. If $\alpha < 1$ and $\beta/(1-\alpha) \leq \epsilon_0$, then set the shadowing distance $\epsilon := \beta/(1-\alpha)$.

Note: If $\alpha \geq 1$ then no shadowing distance can be obtained and no statement can be made about the global error associated with computing a solution to (2.1).

6.2 Numerics

Our code is written using Fortran 77 and compiled and run on a RedHat 8.0 Linux system with 512MB of RAM and one 2.4GHz Intel Pentium 4 processor.

We rely on third-party code packages within our code to provide certain functionality. These are:

• donest.f - Hager/Higham's code for one norm estimation.

• bl3dfac.f, bl3dsol.f - Fortran codes of Keast [30] used with donest.f to factor and solve block tridiagonal linear systems during norm estimation.

• BLAS - basic linear algebra subroutines for matrix-matrix and matrix-vector multiplication.

When solving (4.8) and (4.9) we employ the stiff numerical integrator SODEX ([23], extrapolation code based on the linearly implicit midpoint rule). When integrating, SODEX will determine stepsizes based on the relative and absolute error tolerances which we specify along with an initial stepsize as arguments. At each timestep, we save the solutions generated by SODEX as well as the three entries on the diagonal of $\tilde{A}$ which we are interested in. We will also estimate and save the Lipschitz constants (5.6)–(5.9).

After numerical integration is complete, we move to generate our shadowing result, ϵ, by using algorithm (6.1). All constants which we estimate are based on the data stored during numerical integration. We discuss in the next section how these constants are estimated.

6.3 Implementation Details

6.3.1 Estimation of the Constants in (4.13) – (4.15)

By assuming that the fundamental matrix solution of (4.7) is integrally separated, this implies that the functions along the diagonal of $\tilde{A}$ from (4.9) are integrally separated and, because of this, for our numerical testing, we approximate constants K, J, d, a, γ, and ω using the following equations and ideas.

Define

$$\gamma_H = \sup_t \frac{1}{H} \int_t^{t+H} \tilde{A}(\tau)_{1,1} d\tau, \quad H > 0, \tag{6.1}$$

where $\tilde{A}(t)_{1,1}$ is the $(1,1)$ element of the matrix $\tilde{A}$.

Similarly, define

$$\omega_H = \sup_t \frac{1}{H} \int_t^{t+H} \tilde{A}(\tau)_{p+1,p+1} d\tau, \quad H > 0 \tag{6.2}$$

where $\tilde{A}(t)_{p+1,p+1}$ is the $(p+1, p+1)$ element of the matrix $\tilde{A}$, and

$$a_H = \sup_t \frac{1}{H} \int_t^{t+H} \left[\tilde{A}(\tau)_{p,p} - \tilde{A}(\tau)_{p+1,p+1} \right] d\tau, \quad H > 0. \tag{6.3}$$

To find γ_H, ω_H and a_H numerically, we will fix H such that $0 < H \leq t_{end}/2$ and then compute the sup over all $t \equiv \{t_k\}_{k=0}^M$.

Using the above values, we can find, K, J, and $1/d$ in the following manner:

$$K_H = \sup_{t,s} e^{\int_t^s \left[\tilde{A}(\tau)_{1,1} - \gamma_H\right] d\tau}, \tag{6.4}$$

$$J_H = \sup_{t,s} e^{\int_t^s \left[\tilde{A}(\tau)_{p+1,p+1} - \omega_H\right] d\tau}, \tag{6.5}$$

$$\left(\frac{1}{d}\right)_H = \sup_{t,s} e^{\int_t^s \left[\tilde{A}(\tau)_{p,p} - \tilde{A}(\tau)_{p+1,p+1} - a_H\right] d\tau}. \tag{6.6}$$

As an alternative to employing equations (6.4)–(6.6) for every timestep, we employ the following alternative method to find the supremal values for K, J, and $1/d$:

Compute $K_{H/2}$ as

$$K_{H/2} = e^{\int_t^{t+\frac{H}{2}} \left[\tilde{A}(\tau)_{1,1} - \gamma_H\right] d\tau}, \tag{6.7}$$

for all $t \equiv \{t_k\}_{k=0}^M$. We will set $K = \max\left\{K_{H/2}\right\}$. In a similar manner, we obtain values for J and $1/d$.

6.3.2 Estimation of η_1

In order to estimate $\|D_1^\dagger\|_\infty = \eta_1$, we make use of the fact that the pseudo-right inverse of D_1 can be written $D_1^\dagger = D_1^T(D_1 D_1^T)^{-1}$. This implies $(D_1 D_1^T)(D_1^\dagger)^T = D_1$. Notice that by solving a linear system for a column of $(D_1^\dagger)^T$ we are actually solving for a row of $D_1^\dagger$, which we require to estimate the infinity norm of $D_1^\dagger$.

The norm estimate is done using a method first proposed by Hager [20] and later refined by Higham [27]. Hager's algorithm will calculate the one norm of a given matrix, A, using a simple scheme in which it will multiply Ax or $A^T x$ until the norm is estimated. Note that we are using Hager to calculate $\|(D_1^\dagger)^T\|_1 = \|D_1^\dagger\|_\infty$.

When a request is made to find $(D_1^\dagger)^T x$ or $D_1^\dagger x$ we will multiply $D_1 x = w$ and solve $D_1 D_1^T y = w$ or solve $D_1 D_1^T w = x$ and multiply $y = D_1^T w$, respectively. We take advantage of the fact that our matrix $D_1 D_1^T$ is tridiagonal in solving the systems in the most efficient manner possible.

6.3.3 Simplified Bound on η_2

If we let $h = \min_k(t_{k+1} - t_k)$, then (5.33) becomes,

$$\begin{aligned} \|z_{k+1}\|_\infty &\leq J\left[1 + e^{\omega k h} + \ldots + e^{\omega 2h} + e^{\omega h}\right] \\ &= J\left[1 + e^{(\omega h)^k} + \ldots + e^{(\omega h)^2} + e^{\omega h}\right]. \end{aligned} \tag{6.8}$$

The above sum is a geometric series and can be expressed as

$$J\left[1 + e^{(\omega h)^k} + \ldots + e^{(\omega h)^2} + e^{\omega h}\right] \leq J\frac{1 - e^{(\omega h)^{k+1}}}{1 - e^{\omega h}} \leq J\frac{1}{1 - e^{\omega h}} := \eta_2. \tag{6.9}$$

6.3.4 Estimation of $M_{\tilde{A}}$

During our numerical calculation, we solve for $p+1$ columns of the linear variational equation (4.7). In doing so, we form $\tilde{A} \in \mathbb{R}^{(p+1)\times(p+1)}$. The $(p+1)$st column of $\tilde{A}$ is the first column in the submatrix $\tilde{A}^{(12)}$. We estimate $M_{\tilde{A}}$ based on the formula,

$$M_{\tilde{A}} = \max_k \|\tilde{A}^{(k)}_{p+1}\|_\infty, \tag{6.10}$$

where $\tilde{A}^{(k)}$ is the matrix formed during each step of numerical integration.

Chapter 7

NUMERICAL RESULTS

In this chapter, we present numerical results of our shadowing algorithm applied to several nonlinear IVPs. We have chosen these IVPs because they are known to exhibit integral separateness and are of physical interest in a variety of disciplines. The main goal in our experiments is to obtain shadowing estimates for a long time integration of (2.1). We are also interested in testing our procedure for increasing values of n, in the interest of testing for n large, i.e. high dimensional systems.

The results for each of the examples we consider are for different values of p varied over a fixed mesh determined by n.

Each problem was spatially discretized to yield a first-order system of differential equations which we then solve numerically. For each problem, there are two tables listing the results we obtained. The first table of each pair gives values for K, J, a, γ, ω and $1/d$ from our assumptions (4.13) – (4.15) which we use when bounding α_1, α_2 and α_3 from Theorem 5.1.1. The second table of each pair gives the values which go into satisfying Theorem 4.2.1, our shadowing theorem. If $\alpha < 1$, then the shadowing distance ϵ is assigned, which is our end goal. If assigned, we can say that there is an exact solution to the original problem within ϵ of the computed solution.

7.1 Examples

Example 7.1.1. *The Lorenz equation is given by*

$$\dot{x} = \sigma(y - x),$$

$$\dot{y} = \rho x - y - xz,$$

$$\dot{z} = xy - \beta z,$$

where

$$\bar{x}(t) = \begin{pmatrix} x(t) \\ y(t) \\ z(t) \end{pmatrix} \in \mathbb{R}^3, \quad t \in \mathbb{R}$$

with parameters $\sigma = 10, \rho = 28, \beta = \frac{8}{3}$.

The Lorenz equation is an often cited example studied in dynamical systems. The equations are simple, yet they contain a strange attractor and exhibit chaotic behaviour.

Tables 7.1 and 7.2 give shadowing results for the Lorenz system where we have chosen the shadowing constant $H = 1$ for the estimation of our constants. The results show that we were not able to get a shadowing distance for the case when $p = 2$ and only obtain a shadowing distance when $p = n = 3$.

Example 7.1.2. *The Chafee-Infante reaction-diffusion equation (CIE) is given by*

$$U_t - U_{xx} + \kappa(U^3 - U) = 0, \quad U(t,0) = U(t,1) = 0 \tag{7.1}$$

on $\mathbb{R}^+ \times [0,1]$. *To make the dynamics of the problem more interesting, we use the*

Lorenz ($n = 3$, $t_{end} - t_{start} = 10$, $\delta = 10^{-6}$, $\theta = 10^{-2}$)						
p	γ	K	ω	J	a	$1/d$
2	.63	1.0	$-1.0e01$	1.0	$1.5e01$	1.1
3	.63	1.0	0	1.0	-10.6	1.0

Table 7.1. Bounded growth and integral separation constants for Lorenz.

Lorenz ($n = 3$, $t_{end} - t_{start} = 10$, $\delta = 10^{-6}$)					
p	η	α_1	α_2	α_3	ϵ
2	$4.7e1$	$1.0e-06$	$3.2e-05$	0.3	
3	$9.4e1$	$1.0e-06$	$3.4e-05$	0	$9.4e-05$

Table 7.2. Shadowing theorem values for Lorenz.

initial condition

$$U(0,x) = f(x) = \begin{cases} 0, & 0 \leq x < 1/5 \\ 1, & 1/5 \leq x \leq 2/5 \\ 0, & 2/5 < x < 3/5 \\ 1, & 3/5 \leq x \leq 4/5 \\ 0, & 4/5 < x \leq 1 \end{cases}$$

and parameter $\kappa = 1$.

Reaction-diffusion equations, as a general class of problems, arise in many chemical and biological settings. Solutions to these equations exhibit a wide variety of structures, including pattern formation and traveling waves. The CIE is a scalar reaction-diffusion problem and an example of a dissipative parabolic PDE. The CIE was originally studied as a model of the evolution of the alignments in crystals and Chafee-Infante studied the equation as a bifurcation problem in their work [5].

The CIE was discretized using basic finite differences with Dirichlet boundary conditions. The dimension n can be set arbitrarily ≥ 2.

Tables 7.3 and 7.4 give shadowing results for a 15-dimensional system, where we have chosen $H = 1$ for the estimation of our shadowing constants.

For CIE, we were able to obtain a shadowing distance for all values of p which we considered. This is not entirely surprising as CIE is dissipative and so we would expect the modes of the system to decay with time. The fact that α_3 is quite small for all values of p is what allows us to obtain the shadowing distance in each case.

Chafee-Infante ($n = 15$, $t_{end} - t_{start} = 10$, $\delta = 10^{-6}$, $\theta = 10^{-2}$)						
p	γ	K	ω	J	a	$1/d$
2	−8.8	1.0	−8.5e01	1.0	4.8e01	1.0
3	−8.8	1.0	−1.5e02	1.0	6.4e01	1.0
4	−8.8	1.0	−2.3e02	1.0	7.8e01	1.0
5	−8.8	1.0	−3.2e02	1.0	8.9e01	1.0
6	−8.8	1.0	−4.1e02	1.0	9.6e01	1.0
7	−8.8	1.0	−5.1e02	1.0	10.0e01	1.0
8	−8.8	1.0	−6.1e02	1.0	10.0e01	1.0
9	−8.8	1.0	−7.0e02	1.0	9.6e01	1.0
10	−8.8	1.0	−7.9e02	1.0	8.9e01	1.0
11	−8.8	1.0	−8.7e02	1.0	7.8e01	1.0
12	−8.8	1.0	−9.3e02	1.0	6.4e01	1.0
13	−8.8	1.0	−9.8e02	1.0	4.8e01	1.0
14	−8.8	1.0	−1.0e03	1.0	3.1e01	1.0

Table 7.3. Bounded growth and integral separation constants for Chafee-Infante.

Example 7.1.3. *As a final example, we consider a closed loop thermosyphon. The model for the thermosyphon is a coupled nonlocal ODE/PDE system for the velocity, $v(t)$, and the temperature of the fluid, $T(t,x)$, of the form*

$$\begin{cases} \epsilon v_t + G(v)v = \oint Tf, \quad v(0) = v_0, \\ T_t + vT_x = h(x) + vT_{xx}, \quad T(0,x) = T_0(x), \end{cases} \tag{7.2}$$

Chafee-Infante ($n = 15$, $t_{end} - t_{start} = 10$, $\delta = 10^{-6}$)					
p	η	α_1	α_2	α_3	ϵ
2	3.6	$1.0e-06$	$3.8e-05$	$9.7e-12$	$3.6e-06$
3	3.7	$1.0e-06$	$8.5e-05$	$1.2e-11$	$3.7e-06$
4	7.5	$1.0e-06$	$1.5e-04$	$1.1e-11$	$7.6e-06$
5	1.1e01	$1.0e-06$	$2.3e-04$	$4.0e-10$	$1.1e-05$
6	1.4e01	$1.0e-06$	$3.2e-04$	$1.1e-10$	$1.4e-05$
7	1.8e01	$1.0e-06$	$4.1e-04$	$3.9e-10$	$1.9e-05$
8	2.0e01	$1.0e-06$	$5.1e-04$	$4.6e-11$	$2.0e-05$
9	2.4e01	$1.0e-06$	$6.1e-04$	$5.2e-10$	$2.5e-05$
10	2.8e01	$1.0e-06$	$7.1e-04$	$1.3e-10$	$2.9e-05$
11	3.0e01	$1.0e-06$	$8.0e-04$	$2.6e-10$	$3.1e-05$
12	3.6e01	$1.0e-06$	$8.7e-04$	$3.3e-10$	$3.7e-05$
13	3.7e01	$1.0e-06$	$9.4e-04$	$2.2e-10$	$3.8e-05$
14	3.9e01	$1.0e-06$	$9.8e-04$	$5.5e-11$	$4.1e-05$

Table 7.4. Shadowing theorem values for Chafee-Infante.

with initial conditions v_0 and $T_0(x)$. The parameter ϵ is a positive scalar, $x \in (0,1)$ is the arc length and $\oint = \int_0^1 dx$ denotes integration along the closed path of the circuit. The function $f = dz/dt$ represents the variation in height along the circuit, so f describes the geometry of the loop and the distribution of gravitational forces. The function h represents the heat transfer law across the loop wall. The function $G(v)$ specifies the friction law at the inner wall of the loop and is positive and bounded away from zero; i.e., $G(v) \geq G_0 > 0$.

In engineering, the name thermosyphon is used to denote a loop containing fluid whose motion is driven by the action of several forces such as gravity, buoyancy induced by differences in temperature (natural convection), pumps, etc. Examples of real world thermosyphons are cooling circuits and solar water heaters. Thermosyphons can also represent simplified models for natural convection of fluids

throughout nature (atmospheric, oceanic circulation loops). Thermosyphons are attractive for study because they can give rise to mathematical equations that can be studied with simple laboratory implementations. See, for example, [34].

The discrete model for this equation is obtained by spatially discretizing the PDE system by considering Fourier expansions for f and T in (7.2) and writing the equations for the Fourier coefficients of T. Then, the expansions have been truncated to the first terms, producing a nonlinear system of first order ODEs. The discretization produces either three or five dimensional models where we can add arbitrarily many more contracting dimensions. We follow the discretization given in [34] exactly and refer the reader therein for a detailed description and history of the discretization of this model.

For the numerical results given here, we take $\epsilon = 1$, $G(v) = |v| + 10^{-4}$ and $h(x) = 10^{-2}|x| + 1$. We have chosen our shadowing constant $H = 1$.

Tables 7.5 and 7.6 give shadowing results for a 3-dimensional model in which we have 3 non-contracting modes and can add arbitrarily many more even dimensions, all of which are contracting.

Tables 7.7 and 7.8 give shadowing results for a 5-dimensional model in which we have 5 non-contracting modes and can add arbitrarily many more even dimensions, all of which are contracting.

The results for both of the thermosyphon models are quite interesting. In each case, we explicitly know the value of p (3 and 5 respectively) and it is precisely at these points when we are able to obtain a shadowing distance. In each problem, when we chose p to be less than 3 and 5, we were unable to obtain a shadowing distance because of the fact that α_3 is large in each case as we are including some of the non-contracting modes of the system into its' estimate.

3D-Thermosyphon ($n = 15$, $t_{end} - t_{start} = 2$, $\delta = 10^{-6}$, $\theta = 10^{-2}$)						
p	γ	K	ω	J	a	$1/d$
2	4.8	1.4	$6.1e-01$	1.8	$9.2e-01$	1.0
3	4.6	1.5	-1.0	1.0	1.6	1.8
4	4.3	1.8	-1.0	1.0	$8.1e-05$	1.0
5	4.6	1.5	-1.0	1.0	$9.9e-03$	1.0
6	4.6	1.5	-1.0	1.0	$5.6e-04$	1.0
7	4.5	1.5	-1.0	1.0	$1.6e-02$	1.0
8	4.5	1.6	-1.0	1.0	$2.2e-03$	1.0
9	4.5	1.6	-1.0	1.0	$2.5e-02$	1.0
10	4.4	1.6	-1.0	1.0	$7.9e-03$	1.0
11	4.4	1.6	-1.0	1.0	$4.9e-02$	1.0
12	4.4	1.6	-1.0	1.0	$3.5e-02$	1.0
13	5.0	1.1	-1.0	1.0	$2.1e-01$	1.0
14	4.5	1.8	-4.4	4.8	$2.2e-01$	2.6

Table 7.5. Bounded growth and integral separation constants for the 3D-thermosyphon model.

7.2 Discussion of Results

In each of the three examples that we considered we obtained results which were consistent with what we expected to see given the nature of the systems we were looking at.

For the CIE, we were able to compute a shadowing distance for all values of p because the entire system is, in general, contracting and hence all of the modes decay with time.

For each of the thermosyphon models studied, we knew p explicitly and observed that we were able to obtain a shadowing estimate starting precisely at that value of p. The results for the thermosyphon model are exactly what we would have expected to see and are a good validation of the procedure presented in this thesis.

3D-Thermosyphon ($n = 15$, $t_{end} - t_{start} = 2$, $\delta = 10^{-6}$)					
p	η	α_1	α_2	α_3	ϵ
2	1.3e02	$1.1e-06$	$9.9e-04$	7.2e02	
3	2.2e01	$1.0e-06$	$9.9e-04$	$3.2e-02$	$2.3e-05$
4	2.2e01	$1.1e-06$	$1.4e-03$	$3.9e-02$	$2.3e-05$
5	2.4e01	$1.1e-06$	$1.8e-03$	$5.6e-02$	$2.5e-05$
6	2.2e01	$1.1e-06$	$1.0e-03$	$2.9e-02$	$2.3e-05$
7	2.4e01	$1.1e-06$	$1.1e-03$	$3.1e-02$	$2.4e-05$
8	2.4e01	$1.1e-06$	$2.0e-03$	$5.9e-02$	$2.6e-05$
9	2.2e01	$1.1e-06$	$1.1e-03$	$3.2e-02$	$2.3e-05$
10	2.2e01	$1.1e-06$	$1.1e-03$	$3.0e-02$	$2.3e-05$
11	2.3e01	$1.1e-06$	$1.2e-03$	$3.5e-02$	$2.3e-05$
12	2.3e01	$1.0e-06$	$1.1e-03$	$3.1e-02$	$2.4e-05$
13	2.2e01	$1.1e-06$	$1.0e-03$	$3.0e-02$	$2.3e-05$
14	2.8e01	$1.0e-06$	$9.2e-04$	$6.3e-04$	$2.9e-05$

Table 7.6. Shadowing theorem values for the 3D-thermosyphon model.

5D-Thermosyphon ($n = 15$, $t_{end} - t_{start} = 2$, $\delta = 10^{-6}$, $\theta = 10^{-2}$)						
p	γ	K	ω	J	a	$1/d$
2	5.0	1.3	$2.2e-01$	1.5	$9.1e-01$	1.
3	4.7	1.5	$-4.9e-01$	1.2	1.1	1.6
4	4.5	1.6	-1.0	1.1	$6.0e-01$	1.2
5	5.0	1.2	-1.0	1.0	$1.7e-02$	1.0
6	4.9	1.5	-1.0	1.0	$5.8e-04$	1.0
7	4.9	1.4	-1.0	1.0	$1.6e-02$	1.0
8	4.6	1.7	-1.0	1.0	$2.2e-03$	1.0
9	4.6	1.7	-1.0	1.0	$2.5e-02$	1.0
10	4.6	1.7	-1.0	1.0	$7.9e-03$	1.0
11	4.6	1.7	-1.0	1.0	$4.9e-02$	1.0
12	4.6	1.7	-1.0	1.0	$3.5e-02$	1.0
13	5.1	1.2	-1.0	1.0	$2.1e-01$	1.0
14	4.9	1.6	-4.4	4.7	$2.2e-01$	2.3

Table 7.7. Bounded growth and integral separation constants for the 5D-thermosyphon model.

5D-Thermosyphon ($n = 15$, $t_{end} - t_{start} = 2$, $\delta = 10^{-6}$)					
p	η_2	α_1	α_2	α_3	ϵ
2	7.2e01	$1.1e-06$	$9.2e-04$	5.3	
3	3.2e01	$1.0e-06$	$9.8e-04$	3.5	
4	2.6e01	$2.8e-05$	$1.2e-03$	2.3	
5	3.3e01	$1.1e-06$	$1.6e-03$	$4.4e-04$	$3.5e-05$
6	3.2e01	$1.0e-06$	$1.4e-03$	$2.8e-04$	$3.4e-05$
7	3.1e01	$1.7e-06$	$1.1e-03$	$2.3e-04$	$3.3e-05$
8	3.1e01	$1.2e-06$	$1.4e-03$	$2.3e-04$	$3.3e-05$
9	3.1e01	$1.1e-06$	$1.4e-03$	$4.0e-04$	$3.3e-05$
10	3.1e01	$1.1e-06$	$1.4e-03$	$2.9e-04$	$3.3e-05$
11	3.2e01	$1.1e-06$	$1.4e-03$	$3.7e-04$	$3.4e-05$
12	3.2e01	$1.1e-06$	$1.4e-03$	$2.5e-04$	$3.4e-05$
13	3.3e01	$1.1e-06$	$1.1e-03$	$2.4e-04$	$3.4e-05$
14	2.8e01	$1.0e-06$	$7.9e-04$	$4.2e-04$	$2.9e-05$

Table 7.8. Shadowing constants for the 5D-thermosyphon model.

Chapter 8

CONCLUSIONS

In this thesis we devised a new approach to global error analysis for approximate solutions to IVP ODEs using a shadowing lemma type approach. By considering that the system with which we were dealing was integrally separated we were able to separate the system and obtain shadowing results more efficiently by dealing with the parts of the system separately and taking into consideration the particular dynamics of each part. We were able to achieve a more efficient shadowing estimate by obtaining a shadowing estimate for the non-contracting modes of the system and estimating the error contributed from the rest of the modes. The higher efficiency resulted from having to solve a lower dimensional system of DEs, while still giving enough information to produce a shadowing result.

REFERENCES

[1] L. Ya. Adrianova, Introduction to Linear Systems of Differential Equations, Translations of Mathematical Monographs Vol. 146, AMS, Providence, R.I. (1995).

[2] B. Benettin and A. Giorgilli, "On the Hamiltonian interpolation of near the identity symplectic mappings with application to symplectic integration algorithms," *J. Stat. Phys.* **74** (1994), pp. 1117–1143.

[3] W. J. Beyn, "On the numerical approximation of phase portraits near stationary points," *SIAM J. Numer. Anal.* **24** (1987), pp. 1095–1113.

[4] B. F. Bylov, "On the reduction of systems of linear equations to the diagonal form," *Math. Sb.* **67** (1965), pp. 338–334.

[5] N. Chafee and E. F. Infante, "A bifurcation problem for a nonlinear partial differential equation of parabolic type," *Applicable Anal.* **4** (1974), pp. 17–37.

[6] S. N. Chow, X. B. Lin and K. J. Palmer, "A shadowing lemma with applications to semilinear parabolic equations," *SIAM J. Math. Anal.* **20** (1989), pp. 547–557.

[7] S. N. Chow and K. J. Palmer, "On the numerical computation of orbits of dynamical systems: the higher dimensional case," *J. of Complexity* **8** (1992), pp. 398–423.

[8] B. A. Coomes, "Shadowing orbits of ordinary differential equations on invariant submanifolds," *Trans. AMS* **349** (1997), pp. 203–216.

[9] B. A. Coomes, H. Kocak and K. J. Palmer, "Rigorous computational shadowing of orbits of ordinary differential equations," *Numer. Math.* **69** (1995), pp. 401–421.

[10] P. Constantin, C. Foias, B. Nicolanko and R. Teman, Integral Manifolds and Inertial Manifolds for Dissipative Partial Differential Equations, Springer-Verlag, Berlin (1988).

[11] W. A. Coppel, Dichotomies in Stability Theory, Lecture Notes in Mathematics 629, Springer-Verlag, Berlin (1978).

[12] S. Dawson, C. Grebogi, T. Sauer and J. A. Yorke, "Obstructions to shadowing when a Lyapunov exponent fluctuates about zero," *Phys. Rev. Lett.* **73** (1994), pp. 1927–1930.

[13] L. Dieci and E. S. Van Vleck, "Computation of orthonormal factors for fundamental solution matrices," *Numer. Math.* **83** (1999), pp. 599–620.

[14] L. Dieci and E. S. Van Vleck, "Lyapunov spectral intervals: theory and computation," *SIAM J. Numer. Anal.* **40** (2003) pp. 516–542.

[15] U. Dressler, "Symmetry property of the Lyapunov spectra of a class of dissipative dynamical systems with viscous damping," *Physical Review A*, **38-4** (1988), pp. 2103–2109.

[16] J. E. Franke and J. F. Selgrade, "Hyperbolicity and chain recurrence," *J. Diff. Eqn.* **26** (1977), pp. 27–36.

[17] J. E. Franke and J. F. Selgrade, "A computer method for verification of asymptotically stable periodic orbits," *SIAM J. Math. Anal.* **10** (1979), pp. 614–628.

[18] G. H. Golub and C. F. Van Loan, Matrix Computations, Johns Hopkins University Press, Baltimore, MD (1989).

[19] O. Gonzalez, D. J. Higham and A. M. Stuart, "Qualitative properties of modified equations," *IMA J. of Numer. Anal.* **19** (1999), pp. 169–190

[20] W. Hager, "Condition estimates," *SIAM J. Sci. Stat. Comput.* **5** (1984), pp. 311–316.

[21] E. Hairer, "Backward error analysis of numerical integrators and symplectic methods," *Annals of Numer. Math.* **1** (1994), pp. 107–132.

[22] E. Hairer and C. Lubich, "The life-span of backward error analysis for numerical integrators," *Numer. Math.* **76** (1997), pp. 441–462.

[23] E. Hairer, S. P. Norsett and G. Wanner, Solving Ordinary Differential Equations I: Nonstiff Problems, Springer-Verlag, Berlin (1987).

[24] J. K. Hale, Ordinary Differential Equations, Krieger, Melbourne, FL (1980).

[25] S. Hammel, J. A. Yorke and C. Grebogi, "Do numerical orbits of chaotic dynamical processes represent true orbits?," *J. Complexity* **3** (1987), pp. 136–145.

[26] S. Hammel, J. A. Yorke and C. Grebogi, "Numerical orbits of chaotic processes represent true orbits," *Bull. Am. Math. Soc.* **19** (1988), pp. 465–470.

[27] N. J. Higham, "Algorithm 674: Fortran codes for estimating the one-norm of a real or complex matrix, with applications to condition estimation," *ACM Tran. Math. Soft.* **14** (1989), pp. 381–396.

[28] E. Isaacson and H. B. Keller, Analysis of Numerical Methods, Dover, Mineola, NY (1994).

[29] L. V. Kantorovich and G. P. Akilov, Functional Analysis, Pergamon Press, Oxford, Second Edition (1982).

[30] P. Keast, http://www.mscs.dal.ca/ keast/research/pubs.html, Mathematics and Statistics Department, Dalhousie University, Canada.

[31] G. Meurant, "A review on the inverse of symmetric tridiagonal and block tridiagonal matrices," *SIAM J. Mat. Anal. Appl.* **13** (1992), pp. 707–728.

[32] B. Noble and J. W. Daniel, Applied Linear Algebra, Prentice-Hall, Englewood Cliffs, NJ, Third Edition (1988).

[33] K. J. Palmer, "Shadowing and Silnikov chaos," *Nonlin. Anal. TMA* **27** (1996), pp. 1075–1093.

[34] A. Rodriguez-Bernal and E. S. Van Vleck, "Complex oscillations in a closed thermosyphon," *Inter. J. of Bifurcation and Chaos* **8** (1998), pp. 41–56.

[35] J. M. Sanz-Serna and S. Larsson,"Shadows, chaos, and saddles," *Applied Numerical Mathematics* **13** (1993), pp. 181–190.

[36] T. Sauer and J. A. Yorke, "Rigorous verification of trajectories for computer simulations of dynamical systems," *Nonlinearity* **4** (1991), pp. 961–979.

[37] G. M. Shroff and H. B. Keller, "Stabilization of unstable procedures: the recursive projection method," *SIAM J. Numer. Anal.* **30** (1993), pp. 1099–1120.

[38] A. M. Stuart and A. R. Humphries, Dynamical Systems and Numerical Analysis, Cambridge University Press, Cambridge (1996).

[39] R. Temam, Infinite-Dimensional Dynamical Systems in Mechanics and Physics, Springer-Verlag, Berlin (1988).

[40] E. S. Van Vleck, "Numerical shadowing near hyperbolic trajectories," *SIAM J. Sci. Comp.* **16** (1995), pp. 1177–1189.

[41] E. S. Van Vleck, "Numerical shadowing using componentwise bounds and a sharper fixed point result," *SIAM J. Sci. Comp.* **22** (2001), pp. 787–801.